Journal of Engineering Physics and Thermophysics, Vol. 68, No. 6, 1995

CLASSIFICATION OF HIGHLY DISPERSED POWDERS IN TRAY SEPARATORS

V. A. Naumov and V. P. Yatsenko

UDC 532.529:622.767.55

We carried out a numerical simulation of the motion and classification of micron-sized particles in a tray separator with a nontraditional direction of tray concavity.

Many branches of industry make wide use of materials in a powder state. Powders serve as the basis for the production of, e.g., catalysts, grinding pastes, wear-resistant compounds, etc. Current production imposes very high requirement on the fractional composition of powders, since it influences the quality of products and the efficiency of technological processes. Among the equipment that fractionates powders, pneumatic centrifugal separators have gained a wide acceptance [1, 2]. In contrast to hydraulic separation [3], pneumatic separation does not require drying of the products and can be used to classify materials that should not be wetted according to the technology of production.

Straight-through air classifiers with a quasi-plane eddy zone [1] make it possible to separate powders according to a boundary dimension $\delta \gtrsim 20\ \mu$m. In centrifugal air classifiers (CAC) with a profiled separation zone [2] a decrease in the magnitude of the boundary dimension δ^* to $5-10\ \mu$m was successfully attained without decreasing the efficiency of the process. However, the performance of CAC's is second to that of straight-through air classifiers. Moreover, both types of apparatus ultimately make it possible to obtain only two fractions of the material. It should be noted that this drawback is typical of the majority of apparatus used for separation. In some cases, for example, in preparing grinding pastes and lapping compounds [4], powder fractions with particle size $\delta \approx 5\ \mu$m are needed. The content of desired particles in fractions should attain 70–80%. It has not been possible to attain such products with the aid of the above apparatus. The decrease in the purity of products in the separation of particles of size $\delta \approx 1-10\ \mu$m in these apparatuses is associated with the fact that the trajectories of fine and coarse particles and of the initial material intersect in the zone of separation. This phenomenon is also observed in liquid separators [3] whose trays have traditional concavity facing downward. It is possible to prevent the intersection of trajectories in apparatuses similar to those described in [3], in which specially fabricated trays have their concavities facing upward. The layout of the trays in such an apparatus is shown in Fig. 1. Here, the direction of gas flow is depicted by dashed lines and of the material by dashed-dotted lines. The zone of separation is formed by two adjacent trays. The present authors are unaware of methods for calculating the motion and classifying particles that would take into account the specific features of such a zone.

Suppose that by one method or another the particles of the initial material are supplied to any of the trays, say, the first one. On the tray, rotating with angular velocity Ω, the particles move under the action of frictional f_{fr}, centrifugal f_c, and Coriolis f_C forces. In the gaps between the trays, in addition to f_c and f_C, an aerodynamic drag force f_a acts on the particles. We shall obtain an equation of motion of a single particle along the trays and in the zone of separation. For this purpose, we introduce a fixed spherical coordinate system (θ, φ, R) (see Fig. 1), where φ is the angle of rotation about the vertical axis. The expression for the kinetic energy of a small particle of a material in this system has the form

$$T = \frac{1}{2} m \left(R^2\Omega_\theta^2 + R^2\Omega_\varphi^2 \sin^2\theta + W^2\right), \tag{1}$$

Institute of the Problems of Energy Saving, Academy of Sciences of Ukraine, Kiev. Translated from Inzhenerno-Fizicheskii Zhurnal, Vol. 68, No. 6, pp. 949-953, November-December, 1996. Original article submitted April 13, 1994.

1062-0125/95/6806-0763$12.50

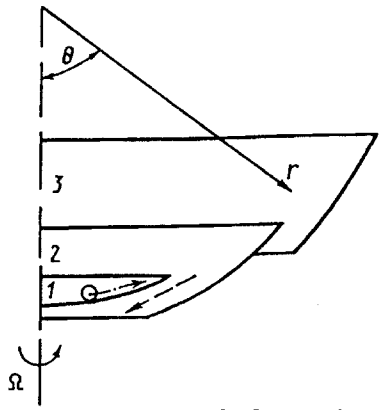

Fig. 1. Layout of trays: 1, 2, 3) numbers of trays.

where m is the mass of the particle; Ω_θ, Ω_φ, W are the components of its velocity along the corresponding axis; $\Omega_\theta = \dot{\theta}$, $\Omega_\varphi = \dot{\varphi}$, $W = \dot{R}$, and the superposed dot indicates the time derivative d/dt.

The change in kinetic energy is described by Lagrange equations of the 2nd kind. As applied to the considered conditions, for the generalized coordinate φ we have

$$\frac{d}{dt}\left(\frac{\partial T}{\partial \dot{\varphi}}\right) - \frac{\partial T}{\partial \varphi} = Q_\varphi , \tag{2}$$

where Q_φ is the generalized force corresponding to φ. We obtain a similar equation for the change in the kinetic energy along the remaining coordinate axes (not given here for the sake of brevity).

Equation (1) yields $\partial T/\partial \varphi = 0$,

$$\frac{d}{dt}\left(\frac{\partial T}{\partial \dot{\varphi}}\right) = m\left[\dot{\Omega}_\varphi R^2 \sin^2\theta + 2\Omega_\varphi R \sin\theta \left(W \sin\theta + R\Omega_\theta \cos\theta\right)\right]. \tag{3}$$

When determining Q_φ, we take into account the action of forces f_a and f_{fr} in Eq. (2). We ignore the gravity force f_g, since it is not involved in possible displacement δ_φ. Then

$$Q_\varphi = 3\pi\delta\rho_g \nu R^2 \left(\Omega_{\varphi g} - \Omega_\varphi\right)\lambda \sin^2\theta + \xi N R_i^2 V^{-1}\left(\Omega - \Omega_\varphi\right)\sin^2\theta . \tag{4}$$

Here ρ, ν are the density and the coefficient of kinematic viscosity; R_i is the radius of the i-th tray; V is the velocity of the relative motion of a particle on a tray; N is the value of the force of a normal reaction acting on the particle from the side of the surface; ξ is the sliding friction coefficient; and λ is a coefficient taking into account the influence of the wall on the magnitude of the aerodynamic drag force (in a free flow $\lambda = 1$).

Equations for V and N have the form

$$V = R_i\left[\Omega_\theta^2 + \left(\Omega - \Omega_\varphi\right)^2 \sin^2\theta\right]^{1/2}, \tag{5}$$

$$N = m\left[R_i\left(\Omega_\theta^2 + \Omega_\varphi^2 \sin^2\theta\right) + g\cos\theta\right], \tag{6}$$

where g is the free-fall acceleration. Substituting expressions (3) and (4) into relation (2), it is possible to obtain an equation of motion of a particle relative to the coordinate φ. Similarly we obtain equations for θ and R. We write the final system of equations of motion in the following dimensionless form:

$$\frac{d\omega_\theta}{d\tau} = \frac{1}{2}\omega_\varphi^2 \sin 2\theta - S\sin\theta - \omega_\theta \Phi - \beta\left(\omega_{\theta g} - \omega_\theta\right), \tag{7}$$

$$\frac{d\omega_\varphi}{d\tau} = \left(1 - \omega_\varphi\right)\Phi - 2\omega_\varphi\left(\omega_\theta \operatorname{ctg}\theta + \frac{w}{r}\right) - \beta\left(\omega_{\varphi g} - \omega_\varphi\right), \tag{8}$$

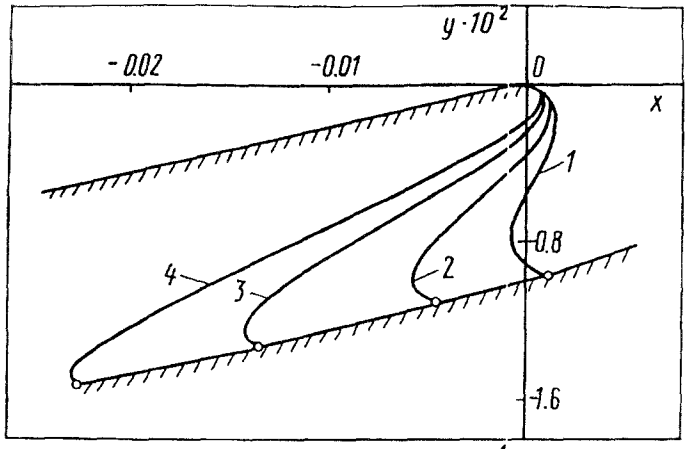

Fig. 2. Trajectories of a particle at $Re_\delta = 0.98 \cdot 10^{-4}$: 1) $Re_u = 33.3$; 2) 60; 3) 100; 4) 140. x, y, mm.

$$\frac{dw}{d\tau} = r(\omega_\theta^2 + \omega_\varphi^2 \sin^2\theta) - \beta w + S\cos\theta - A, \tag{9}$$

where

$$\Phi = \xi \frac{[(\omega_\theta^2 + \omega_\varphi^2 \sin^2\theta) r_i + S\cos\theta] r_i}{[\omega_\theta^2 + (1-\omega_\varphi)^2 \sin^2\theta]^{1/2}}, \quad A = \frac{N}{mR_1\Omega},$$

$$S = \frac{g}{R_1\Omega^2}, \quad \beta = \frac{18\lambda\rho_g}{\rho_p Re_\delta}, \quad Re_\delta = \frac{\Omega\delta^2}{\nu},$$

ρ_p is the particle density; $\tau = t\Omega$, $\omega_\theta = \Omega_\theta/\Omega$, $\omega_\varphi = \Omega_\varphi/\Omega$, $w = W/(R_1\Omega)$, $r = R/R_1$.

If a particle is located on the surface of the i-th tray, then $r = r_i = \text{const}$, $w = 0$, and Eq. (9) is reduced to Eq. (6). In the gaps between the trays $\Phi = 0$.

At the initial time moment ($\tau = 0$)

$$\theta = \theta_0, \quad \omega_\theta = 0, \quad \varphi = 0, \quad \omega_\varphi = 0, \quad r = 1. \tag{10}$$

System of Eqs. (7)-(9) with initial conditions (10) was solved numerically by the Runge-Kutta method. The angular velocities of the gas in the rotating channels were according to [2]. The gas velocity profile in the channels was assumed to be parabolic. Below, we present some of the results of a numerical investigation into the dynamics of particles at the first stage of separation. Here, the stage of separation is understood to be the surface of the tray and the annular air gap (separation zone) between the trays.

The trajectories of the motion of particles in the radial plane of the separation channel at $Re_\delta = 0.98 \cdot 10^{-4}$ are presented in Fig. 2 for different values of the Reynolds number $Re_u = V_1 R_1/\nu$. Here, V_1 is the mean velocity of the gas in the annular channel between the 1st and 2nd trays.

The characteristic S-like form of the curves is attributable to the specificity of the action of forces in a rotating channel. At the center of the channel the linear velocity of gas attains a maximum value and the angular velocity $\omega_{\varphi g}$ a minimum value. Therefore, here the aerodynamic force (the last term on the right-hand side of Eq. (7)) is large, and the centrifugal force (the first term on the right-hand side of Eq. (7)) is small. The particle is entrained by the gas flow to the axis of rotation.

As the gas approaches the surface of the second tray, its linear velocity decreases, and the angular velocity increases. In this region the centrifugal force prevails. Accordingly, the trajectory of the particle deviates from the axis of rotation.

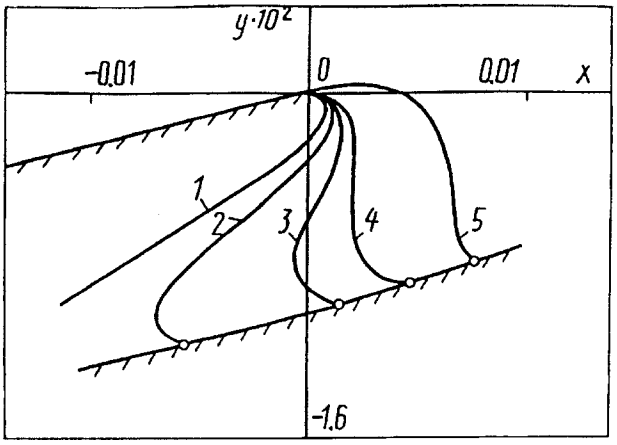

Fig. 3. Trajectories of a particle at Re_u = 33.3: 1) $Re_\delta = 3.2 \cdot 10^{-5}$; 2) $5 \cdot 10^{-5}$; 3) $9.8 \cdot 10^{-5}$; 4) $2 \cdot 10^{-4}$; 5) $8 \cdot 10^{-4}$.

As Re_u increases, the point of deposition of the particle on the surface of the second tray shifts to the axis of rotation. Having reached the surface of the tray, the particle starts to move from the axis of rotation under the action of the centrifugal force.

The trajectories of differently sized particles at Re_u = 33.3 are shown in Fig. 3. As Re_δ decreases, the aerodynamic drag force per unit mass of the particle increases (the dimensionless quantity β in Eq. (7)-(10)), whereas the remaining coefficients in the equations do not change. Fewer inertial particles are deposited on the surface of the trays closer to the axis of rotation. Particles smaller than a certain size δ^* are carried away from the channel by the gas flow (curve 1 in Fig. 3).

A practically important conclusion which follows from the analysis of these results is that the trajectories of fine and large particles do not intersect in the zone of separation. Moreover, with small differences in the sizes of particles, their trajectories are greatly spaced (see Fig. 3), which should increase the efficiency of particle separation.

The second important advantage of the considered method of separation is the possibility of obtaining simultaneously several fractions of a material, since the number of trays can be rather large. This problem cannot be solved in the well-known apparatus [1, 2].

NOTATION

δ, m, particle size and mass; ρ, density; ν, coefficient of kinematic viscosity; f, force; T, kinematic energy; t, time; θ, φ, R, spherical coordinates; Ω, speed of tray rotation; Ω_θ, Ω_φ, W, components of velocity vector; R_1, radius of the first tray; y, x, longitudinal (parallel to the axis of rotation) and transverse distance from the edge of the tray; g, free fall acceleration; $Re_\delta = \Omega\delta^2/\nu$, $Re_u = V_1 R_1/\nu$, Reynolds number. Subscripts: g, gas; i, number of tray.

REFERENCES

1. V. E. Mizonov and S. G. Ushakov, Aerodynamic Classification of Powders [in Russian], Moscow (1989).
2. M. I. Shilyaev, Hydrodynamic Theory of Rotational Separators [in Russian], Tomsk (1983).
3. I. V. Lyskovtsov, Separation of Liquids in Centrifugal Apparatus [in Russian], Moscow (1968).
4. Yu. I. Nikitin, Technology of Production and Control of the Quality of Diamond Powders [in Russian], Kiev (1984).